

The magnetic DA white dwarfs

D. T. Wickramasinghe and Brian Martin *Department of Applied Mathematics, School of General Studies, Australian National University, P.O. Box 4, ACT 2600, Canberra, Australia*

Received 1978 December 21; in original form 1978 August 1

Summary. Theoretical hydrogen line and continuum spectra are computed for magnetic white dwarfs for a range of parameters assuming centred and off-centred field distributions. The results are compared with the observations of the three known magnetic DA white dwarfs GD 90, G 99-47 and BPM 25114. We find that in each case, a centred or off-centred dipole model can be found which gives reasonable agreement with available spectrophotometric data, continuum circular polarization data and spectropolarimetric data. In particular, contrary to the conclusions of some previous investigators, we find no significant discrepancy between observed values of continuum polarization and theoretical values computed on the basis of the standard magnetoabsorption theory.

1 Introduction

Magnetic white dwarf stars can be divided broadly into two groups. The first group consists of stars which show strong polarization and which exhibit spectroscopic features which are unidentified or have uncertain identifications. It seems likely that the spectra of these objects arise from regions of magnetic field strength in excess of roughly 10^8 G, fields at which the theory for the Zeeman effect in the appropriate atomic lines (usually H or He) or molecular bands (usually C_2 or CH) has not been fully developed. Cyclotron absorption could also be important in the optical region of some of these high-field magnetic white dwarfs, giving rise to peculiar absorption features (Wickramasinghe & Martin 1978; Martin & Wickramasinghe 1979a). The second group consists of magnetic white dwarfs which exhibit spectra with identifiable Zeeman structure in atomic or molecular features, usually at lower field strengths. The best known examples of this group are the three magnetic DA white dwarfs GD 90 (Angel *et al.* 1974), G 99-47 (Liebert, Angel & Landstreet 1975) and BPM 25114 (Wickramasinghe & Bessell 1976; Wickramasinghe, Whelan & Bessell 1977), with estimated surface field strengths ranging from roughly 5×10^6 G to 4×10^7 G. These objects are of particular interest since at these lower field strengths the Zeeman effect in

hydrogen and the magnetic dichroism for the appropriate sources of continuous opacity have been worked out in sufficient detail to enable realistic models to be constructed.

In a previous paper (Martin & Wickramasinghe 1978) we presented results of a first attempt to construct detailed models for magnetic DA white dwarfs using non-grey atmospheres and allowing for polarization both in the continuum and in the lines. We discussed a centred dipole model for the southern magnetic DA white dwarf BPM 25114 and showed that good agreement could be obtained with the spectrophotometric observations, but were unable to test predictions of polarization due to the lack of suitable observational data. The availability of good quality polarization and spectroscopic data on the remaining two known magnetic DA white dwarfs GD 90 and G 99-47 places stronger constraints on possible models. In this paper we present a detailed analysis of these two objects and show that good agreement can be achieved with all published observations by assuming centred or off-centred dipole field distributions. We also rediscuss our model for BPM 25114.

2 The models

2.1 ASSUMPTIONS

A detailed account of the assumptions involved in the construction of our models has been given by Martin & Wickramasinghe (1978). We summarize below the basic features of the models, and discuss in detail only the modifications which have since been made to them.

(1) All models have been constructed on the assumption that the pressure and temperature structure of the atmosphere are unaltered by the presence of the magnetic field. The zero-field hydrogen line blanketed white dwarf model atmospheres are taken from Wickramasinghe (1972) and Wickramasinghe, Cottrell & Bessell (1977).

(2) The radiative transfer equations are formulated in terms of Stokes parameters and solved numerically at each wavelength of interest. The numerical technique used in the present computations is discussed by Martin & Wickramasinghe (1979b) and shown to yield accurate results both in the continuum and in the cores of strong lines for a variety of temperature structures. This technique is superior to that used in Martin & Wickramasinghe (1978), particularly in the cores of strong lines such as $H\alpha$, and the resulting modifications to our model of BPM 25114 are discussed in Section 3.3 below.

Polarization in the continuum has been included using the theories of Kemp (1977) and Lamb & Sutherland (1974). The Balmer lines ($H\alpha$, $H\beta$, $H\gamma$ and $H\delta$) were computed using Kemic's (1974a) calculations of the Zeeman effect. All lines were Stark broadened using the Griem (1964) theory. However, we note that the standard Stark broadening theory will cease to be applicable when l degeneracy is removed so that it is likely that the Stark effect has been overestimated at high fields in the present calculations.

(3) Centred dipole and off-centred dipole field distributions are assumed. The free parameters in the models are the effective temperature T_e , gravity g , dipole field strength B_d , the ratio d/R of the dipole's displacement from the centre of the star to the star's radius, and the angle i between the line of sight and the magnetic axis. When the dipole is off-centred, its direction is assumed to lie along the line through the centre of the star and the dipole itself. Therefore the field strengths at the two poles are $B_d(1 - d/R)^{-3}$ and $B_d(1 + d/R)^{-3}$. With this notation a positive value of d/R corresponds to a field geometry in which the stronger pole has positive polarity with field lines going out of the star.

In previous attempts at investigating magnetic white dwarfs, different approaches have

been used for the analysis of line data (spectroscopic and spectropolarimetric) and of continuum circular polarization data. The models of Liebert *et al.* (1975) and Wegner (1977) which deal with the first problem, are based on an exact solution to the radiative transfer equations valid only for a constant B (Planck function) gradient atmosphere with constant ratio of line to continuum opacity with depth. A similar approach has been adopted by Kemic (1974b) and Borra (1976). We find that the computed spectrum is very sensitive to atmospheric structure and that the use of more realistic non-grey atmospheres gives results in better agreement with observations. The second problem, namely that of continuum polarization, has been dealt with by all investigators (e.g. Liebert *et al.* 1977, Brown *et al.* 1977) by using the appropriate magnetic dichroism theory combined with results from an approximate method of solution of the radiative transfer equations following Shipman (1971). This approach is likely to give reasonable results only under very limited conditions, and is discussed critically in Martin & Wickramasinghe (1979b). The major advantage of the method of analysis adopted in this paper is that we are able to discuss continuum and line data in the framework of a single model in a self-consistent manner. Such an approach is important in an analysis of the type attempted in this paper, particularly since the validity of the more basic assumption that the magnetic field does not influence the structure of the atmosphere still needs to be investigated.

2.2 REPRESENTATIVE RESULTS

We first present results for a series of models to illustrate a number of important effects which should be observable in magnetic DA white dwarfs. A zero-field model atmosphere with $T_e = 12\,000\text{ K}$, $\log g = 8.0$ is used for the atmospheric structure. In Figs 1, 2 and 3 are presented the intensity and circular polarization for models with $i = 0^\circ$, 45° and 90° respectively; in each figure $d/R = 0$ and $B_d = 5 \times 10^6\text{ G}$, 10^7 G and $2 \times 10^7\text{ G}$.

We note that for a given angle of viewing i and field strength, the quadratic Zeeman effect in the Balmer lines becomes progressively more important with an increase in the upper principal quantum number n . In particular, the calculations show that for $B_d \geq 2 \times 10^7\text{ G}$, H δ becomes unrecognizable as an individual line for a centred dipole field geometry*. This effect results from the strong n -dependence of the shift in the energy levels of hydrogen in the quadratic Zeeman effect, and has been discussed previously by Kemic (1974b) and various other investigators.

The second effect which is apparent from a comparison of Figs 1, 2 and 3 is that for a given dipole field strength B_d , the lines become less magnetically broadened as i increases from 0° to 90° . This results from the larger effective spread in field strength for pole-on viewing in comparison to equator-on viewing for a centred dipole field distribution.

The results of decentering the dipole by 20 per cent ($d/R = 0.2$) along the polar axis is shown in Figs 4, 5 and 6, for $i = 0^\circ$, 45° and 90° respectively. The intrinsic strengths of the dipoles are taken to be the same as for the sequence of centred dipole models of Figs 1, 2 and 3. The figures for the off-centred dipoles can be understood in terms of mean field strength and effective spread in field strength as a function of i as for the centred dipole models. In comparison to the centred dipole models, the decentred dipole models range from being considerably less uniform in field strength at $i = 0^\circ$ to considerably more uniform at $i = 180^\circ$ (not shown). A variety of spectra exhibiting different degrees of magnetic broadening, as shown in Figs 4 to 6, are thus to be expected.

* The results for H δ for $B > 10^7\text{ G}$ and for H γ for $B > 2 \times 10^7\text{ G}$ are based on extrapolation in Kemic's (1974a) tables and will require modification when more detailed calculations become available.

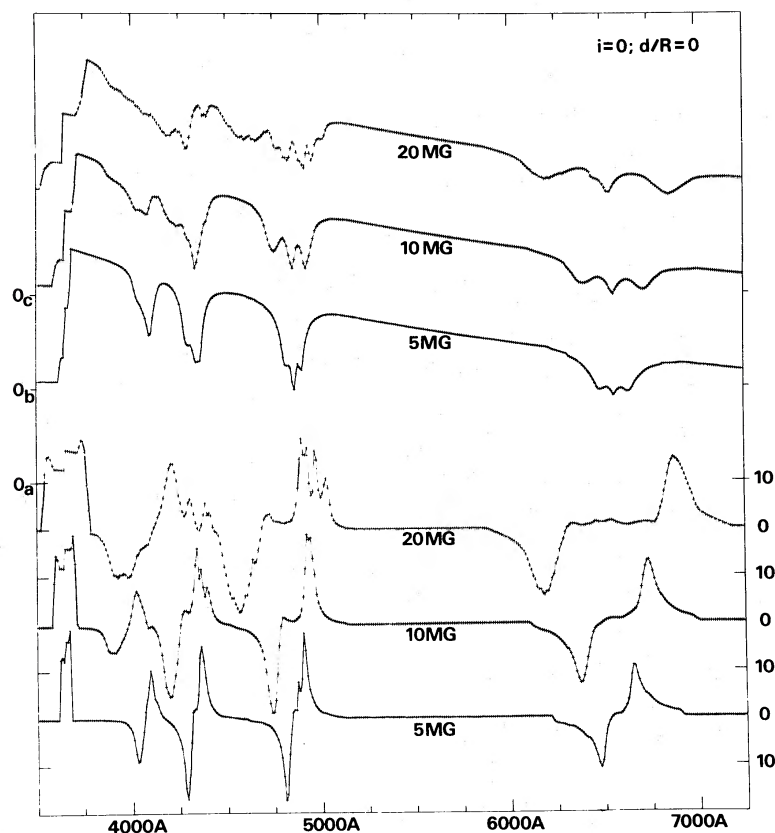


Figure 1. Flux f_p and circular polarization for a model 12 000 K magnetic white dwarf. The curves are identified by their magnetic fields in 10^6 gauss (MG). The bottom three curves represent circular polarization; the scales on the right have units of per cent, with positive polarization values upwards. The top three curves represent flux in arbitrary units; the zeros of these three curves are indicated on the left (0_a , 0_b , 0_c). The other parameters are indicated in the top right corner: the viewing angle is pole-on ($i = 0^\circ$), and the magnetic dipole is centred ($d/R = 0$).

The predicted wavelength dependence of circular polarization is also shown in Figs 1 to 6. Note in particular the strong continuum circular polarization features near the Balmer limit, first predicted by Lamb & Sutherland (1974), and which should be detectable in GD90 (see below). We expect both the intensity and circular polarization data to be somewhat smoother than computed near the Balmer limit due to the opacity from the higher Balmer lines which has not been included.

The complex wavelength dependence of circular polarization in the lines arises as a combination of various effects. We note that a σ^+ (or σ^-) component of a line can contribute both positive and negative circular polarization if it arises from regions with opposite sense of longitudinal magnetic field. For a field distribution which changes rapidly in intensity and direction over the stellar disc, the averaging process results in complex polarization spectra, particularly at high fields when overlapping between components of different lines becomes important. A qualitative discussion of H α polarization using these effects has been given by Borra (1976). We simply note that the details of the circular polarization spectra are strongly dependent on field geometry and provide a powerful method for probing the field structure of magnetic white dwarfs.

For each model we have computed average values of circular polarization V over the wavelength region $\lambda\lambda$ 3500–5500 Å (Table 1). These results include line and continuum polarization and should be directly comparable with broad band polarization observations.

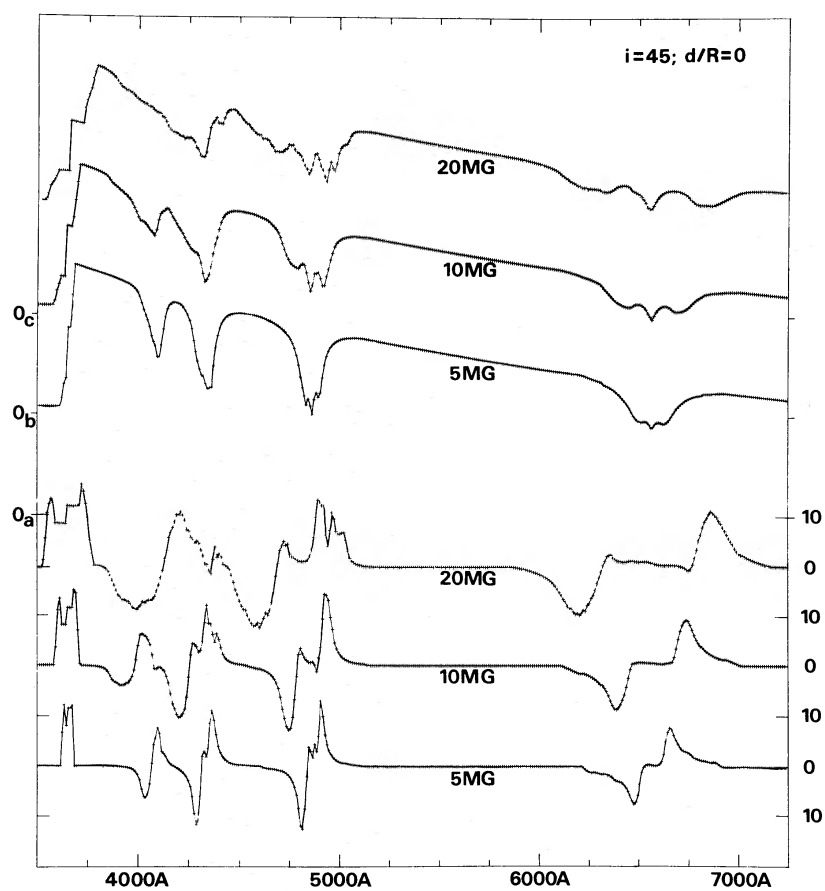


Figure 2. As Fig. 1, except for viewing angle $i = 45^\circ$.

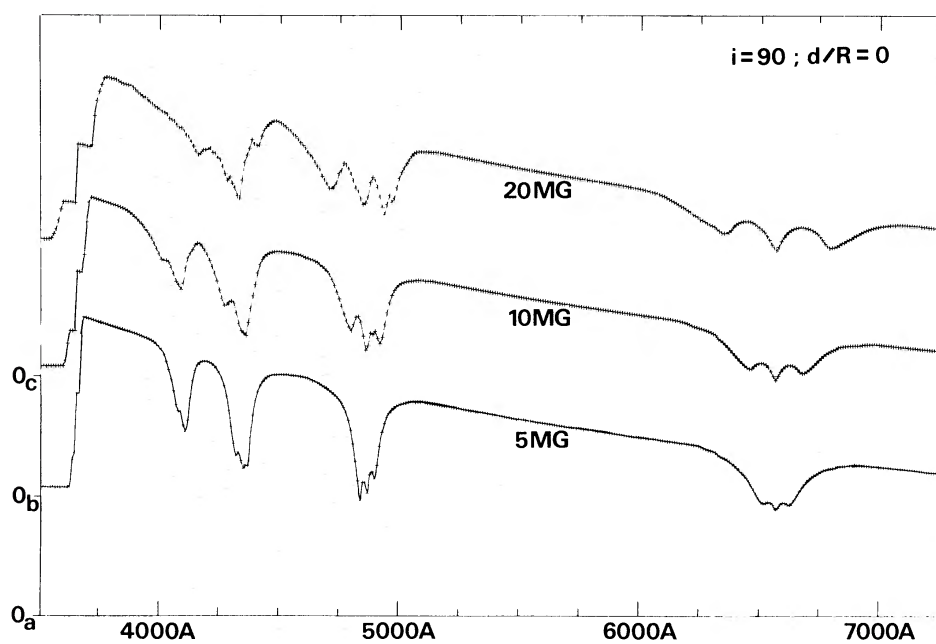


Figure 3. As Fig. 1, except for viewing angle $i = 90^\circ$. The circular polarization values are all equal to zero, and are not shown.

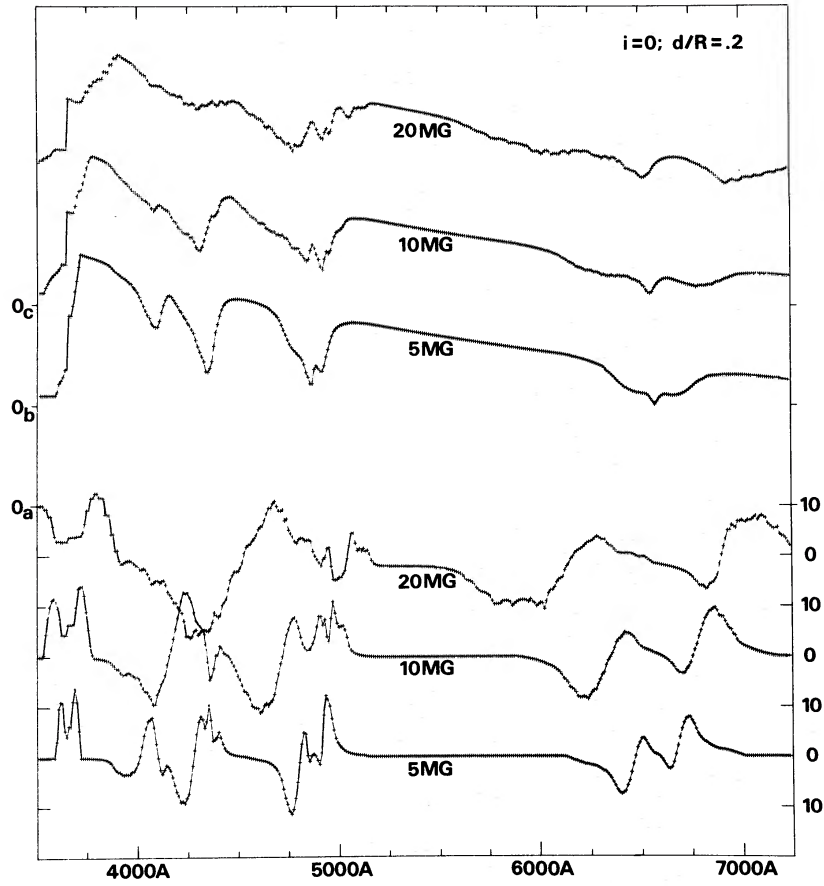


Figure 4. As Fig. 1, except that the magnetic dipole is offset by 20 per cent ($d/R = 0.2$).

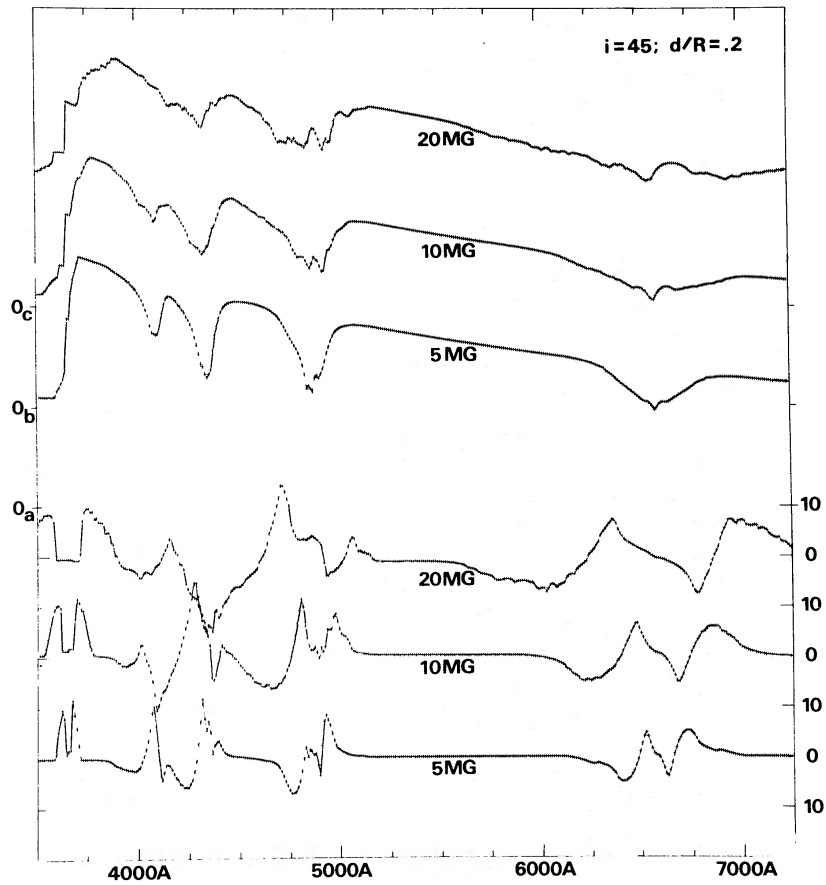


Figure 5. As Fig. 4, except for viewing angle $i = 45^\circ$.

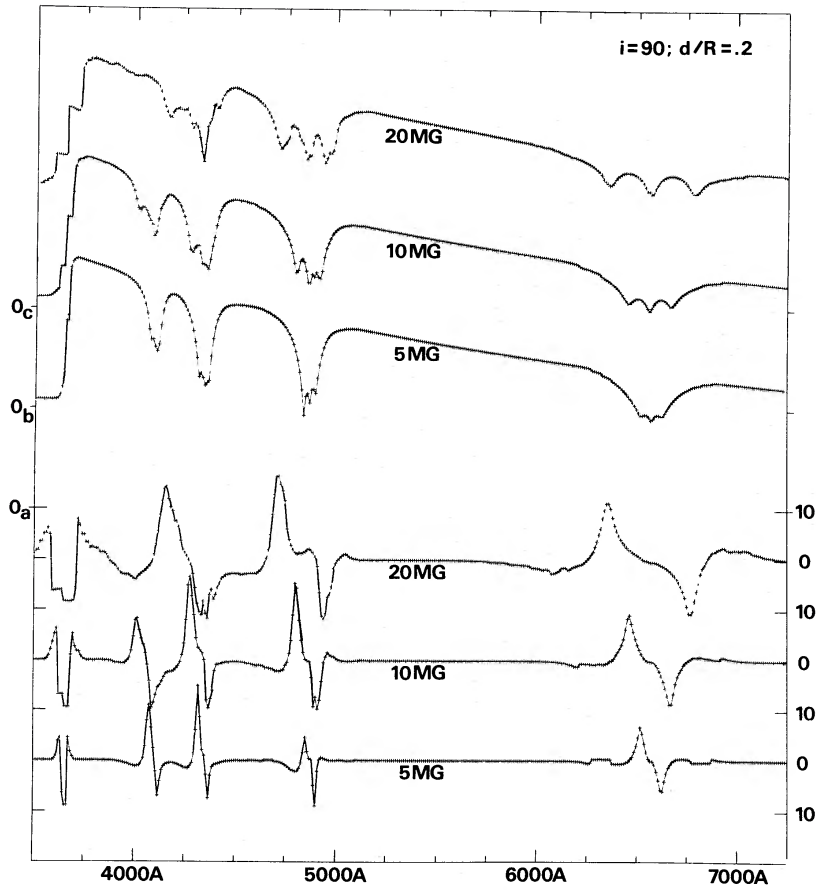


Figure 6. As Fig. 4, except for viewing angle $i = 90^\circ$.

Table 1. Mean computed polarizations for models in Figs 1 to 6.

B_d (gauss)	d/R	i ($^\circ$)	$\bar{V}(\lambda\lambda 3500-5500 \text{ \AA})$ (per cent)
5×10^6	0	0	-0.12
		45	-0.09
		90	0
	0.2	0	-0.19
		45	-0.20
		90	-0.12
10^7	0	0	-0.25
		45	-0.19
		90	0
	0.2	0	-0.25
		45	-0.22
		90	-0.04
2×10^7	0	0	-0.29
		45	-0.26
		90	0
	0.2	0	-0.63
		45	-0.40
		90	-0.06

3 The analysis

3.1 GD 90

GD90 was the first DA white dwarf found to exhibit resolvable Zeeman structure in the Balmer lines (Angel *et al.* 1974). These authors published digicon data in the wavelength interval $\lambda\lambda$ 3900–5100 Å showing the wavelength dependence of both intensity and circular polarization. We use these results in the present investigation, noting that the observed resolution (~ 25 Å) is lower than our adopted theoretical resolution of 10 Å.

Broad-band circular polarization measurements in the wavelength region $\lambda\lambda$ 3500–5500 Å by Angel *et al.* (1974) yielded a null result of $V = -0.03 \pm 0.15$ per cent. More recently Brown *et al.* (1977) have published a value of $V = -0.12 \pm 0.08$ per cent as an average of their own observations and those of Angel *et al.* (1974). They also give an upper limit of 2 per cent for the linear polarization in the V band.

The colours of GD 90 ($U-B = -0.63$, $B-V = 0.22$) (Eggen 1968) suggest an effective temperature $T_e \approx 12\,000$ K. Greenstein (1974) gives a value of $T_e \approx 15\,000$ K based on multi-channel photometric observations. We adopt as our zero-field model a $T_e = 12\,000$ K, $\log g = 8.0$ DA model from Wickramasinghe (1972). The result of using the higher value of 15 000 K is also briefly discussed below. The helium abundance is assumed to be normal, which is consistent with the non-detection of helium lines in GD 90.

Three sets of models with $d/R = 0, 0.1$ and 0.2 were constructed in an attempt to match the observed spectroscopic and polarimetric data on GD 90. The best overall agreement with observations was achieved for an off-centred dipole model with $d/R = -0.1$. The parameters of this model and of the best fitting $d/R = 0$ model are listed in Table 2. The models were selected using a combination of the following criteria.

(1) Wavelength agreement between theory and observations of the components $H\beta$, $H\gamma$ and $H\delta$. Good agreement was achieved for all components with the exception of the σ^+ absorption component of $H\beta$ (λ 4920) (Fig. 7). We compute this component to be at approximately 4910 Å and 4905 Å for the centred and off-centred dipole models respectively, which should be compared with the observed value of 4918 Å. Inspection of Kemic's (1974a) tables suggests that this discrepancy most probably arises from errors introduced by interpolation for the $\sigma^+ 2p(-1) - 4d(-2)$ component which reaches its maximum blueward shift at a field strength in the range $7 \times 10^6 \text{ G} < B < 2 \times 10^7 \text{ G}$.

The structure of $H\delta$ is not apparent in the low-resolution digicon data, although it is clearly present in the spectroscopic data also published in Angel *et al.* (1974). We have chosen not to present a direct comparison with the higher resolution spectroscopic data since these data were not available on an intensity scale.

(2) Agreement between the theoretical and observed spectropolarimetric data. The degree of success achieved in this respect can be judged from Fig. 7. The off-centred dipole

Table 2. Model predictions for GD 90.

B_d (gauss)	d/R	i ($^\circ$)	$\bar{V}(\lambda\lambda$ 3500–5500 Å) (per cent)
* 9×10^6	0	105	0.07
9×10^6	-0.1	120	0.15
* 9×10^6	-0.1	90	0.02
9×10^6	-0.1	60	-0.11

* Best-fitting models as discussed in text.

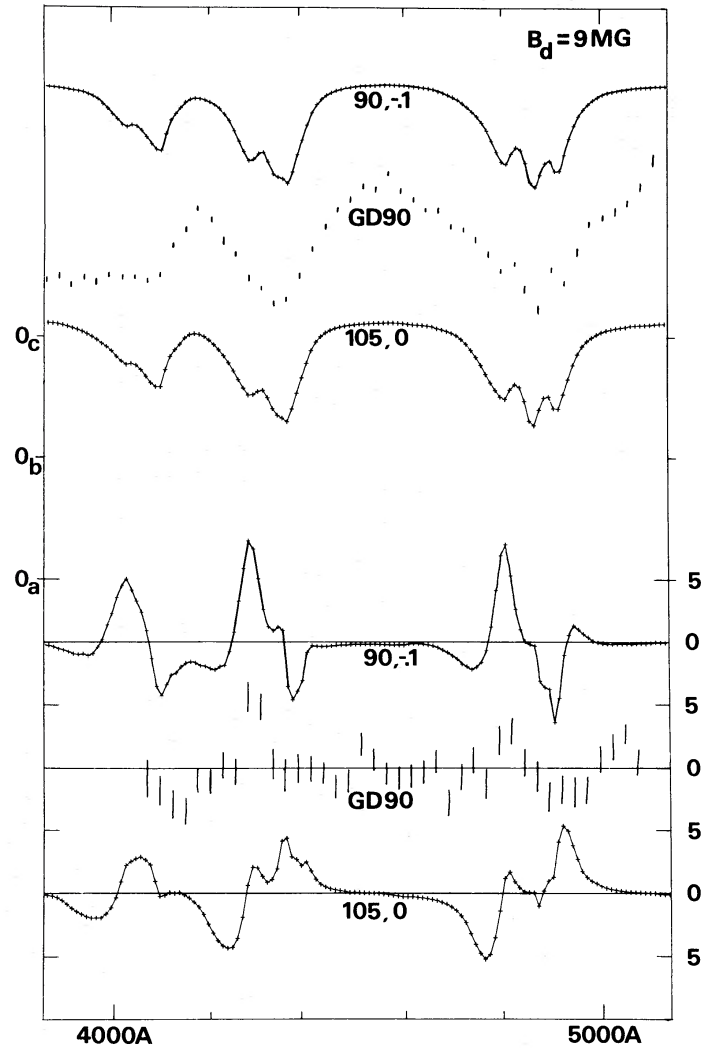


Figure 7. Observed and theoretical fluxes and circular polarization for GD 90. There are three sets of values presented: (a) a model 12 000 K magnetic white dwarf, dipole strength $B_d = 9 \times 10^6$ gauss (9 MG), viewing angle $i = 105^\circ$, centred dipole ($d/R = 0$); (b) observations of magnetic DA white dwarf GD 90 from Angel *et al.* (1974); (c) a model 12 000 K magnetic white dwarf, dipole strength $B_d = 9$ MG, viewing angle $i = 90^\circ$, dipole offset by -10 per cent ($d/R = -0.1$). The bottom three curves represent circular polarization for (a), (b) and (c), from the bottom up respectively; the scales on the right have units of per cent, with *negative* polarization values upwards. The top three curves represent flux multiplied by frequency, in arbitrary units; the zeros of these three curves are indicated on the left (0_a , 0_b , 0_c). The values of the parameters i and d/R are indicated next to the theoretical curves, whose flux values in the continuum are normalized to those of the observed spectrum (b).

model with $i = 90^\circ$ has a polarization spectrum which is very similar to that observed. For this model the observed sign of polarization of the σ^- components of H β and H γ requires the stronger pole to have negative polarity with field lines going into the star. In our notation this corresponds to $d/R = -0.1$. The strong circular polarization features which correspond to observations arise from the central (equatorial) weak field regions of the visible stellar disc which have a net longitudinal field component pointing towards the observer for i near 90° . The contribution from the regions near the stronger pole can be seen in the models as weak wings of opposite sense of polarization superimposed on each of the σ^+ and σ^- components. Although this model can explain the general features of the observed

polarization spectrum, it remains to be seen whether more detailed agreement can be achieved when better data become available.

For the centred dipole case we were unable to achieve good agreement with the observed wavelength dependence of circular polarization. Indeed, it is not even clear which viewing aspect gives best agreement. The polarization spectrum shown in Fig. 7 corresponds to a viewing aspect in which the pole of negative polarity points towards the observer ($i > 90^\circ$). The value of i was selected to give the observed magnitude (about 5 per cent) of circular polarization in the lines. In general these models predict broad circular polarization features for both the σ^+ and σ^- components which are not in accordance with the observations.

(3) Agreement between the observed and theoretical values of broad band ($\lambda\lambda 3500\text{--}5500\text{ \AA}$) circular polarization. This criterion is satisfied by both sets of models if we use the observations of Angel *et al.* (1974), who give $V = -0.03 \pm 0.15$ per cent. On the other hand the value of $V = -0.12 \pm 0.08$ per cent given by Brown *et al.* (1977) as an average overall available observations is only marginally consistent with the off-centred model for $i = 90^\circ$. This is perhaps not surprising, since like BPM 25114 (Martin & Wickramasinghe 1978) and Feige 7 (Liebert *et al.* 1977), GD 90 is likely to be an oblique rotator, and the different sets of observations in V and the spectropolarimetric data need not correspond to the same viewing aspect. On the basis of our analysis, we would expect i to oscillate about 90° with possible associated changes in the sign of polarization. The theoretical continuum and line polarization spectra for the best-fitting off-centred dipole model for different viewing aspects are shown in Fig. 8. The corresponding values of V are given in Table 2. A variation

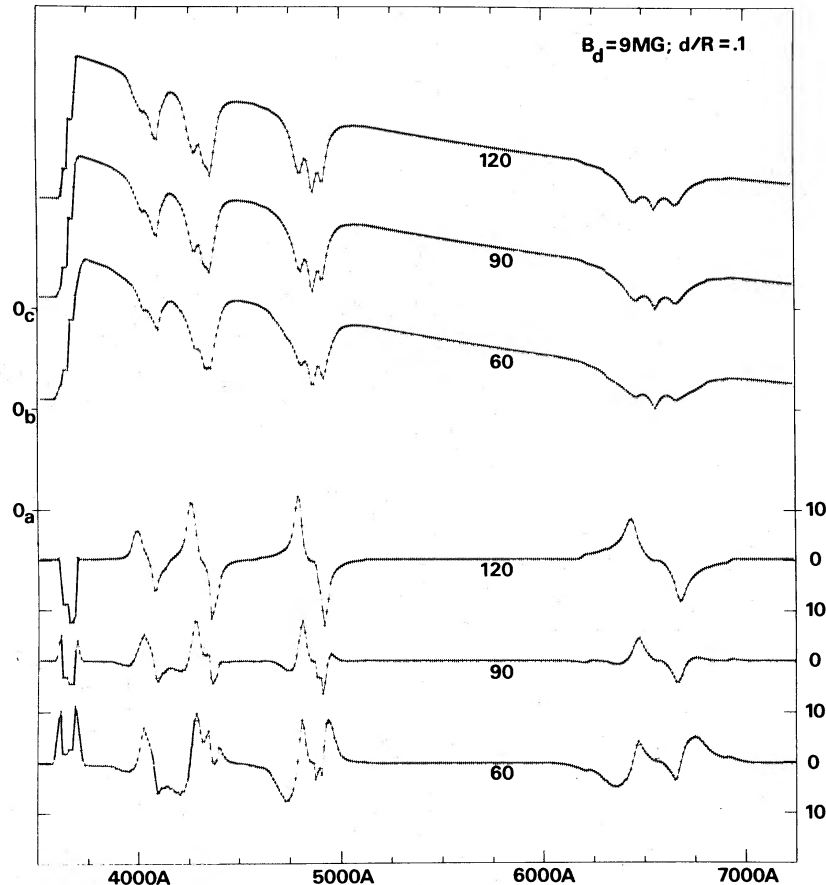


Figure 8. As Fig. 1, except that all curves are for dipole magnetic field strength $B_d = 9$ MG, dipole offset by 10 per cent ($d/R = 0.1$), and viewing angle $i = 60^\circ, 90^\circ$ and 120° as indicated.

in i of $\pm 30^\circ$ during a rotation period would accommodate all available broad band circular polarization observations.

It is evident from Fig. 7 that the observed central depths are larger than the computed values in all cases. The adopted value of effective temperature ($T_e = 12\,000$ K) is near the optimum for producing the strongest Balmer lines in DA white dwarfs. Since Greenstein's (1974) MCP data suggests an even higher value of T_e ($\approx 15\,000$ K), we are led to the conclusion that contrary to our assumption, the magnetic field has an effect on the atmospheric structure. (A model constructed with parameters $T_e = 15\,000$ K, $\log g = 8.0$, $d/R = -0.1$, $B_d = 9 \times 10^6$ G, $i = 90^\circ$ gave polarization and line spectra very similar to the lower temperature model discussed in this paper.) There are two ways in which this could come about.

The magnetic field could have an indirect influence on the atmospheric structure through increased line blanketing caused by the large number of Zeeman components which absorb over a wide wavelength region. A result of this excess line absorption would be the modification of the temperature structure of the upper atmosphere ($\tau \lesssim 0.01$). The zero-field models we have used are hydrogen-line blanketed and already have a structure which differs markedly from the grey temperature distribution at low optical depths. The ratio R of the surface to effective temperature, which gives some measure of the effect of line blanketing and departure from greyness, has values of 0.84 and 0.69 for the grey and $T_e = 12\,000$ K zero-field line-blanketed models respectively. We expect that steepening the surface ($\tau \lesssim 0.01$) temperature gradient by reducing R further will have the desired effect of increasing the central depths to nearer the observed values. A similar result holds for the $T_e = 15\,000$ K model.

A second possibility is that the magnetic field has a direct effect on the hydrostatic equilibrium of the atmosphere. A discussion of this possibility is beyond the scope of the present investigation, but will have to be included for a fine analysis of this object.

3.2 G 99-47

G 99-47 was initially classified as a DC white dwarf by Greenstein, Gunn & Kristian (1971) on the basis of blue spectra. The star was discovered to be circularly polarized with a mean ($\lambda\lambda 3500\text{--}5500$ Å) V of 0.45 per cent by Angel & Landstreet (1972), and subsequent spectropolarimetric observations resulted in the detection of a feature at $\lambda 6542 \pm 5$ Å which was identified as the (strongest) π component of H α shifted by the quadratic Zeeman effect in a mean field of 1.5×10^7 G (Liebert *et al.* 1975). These authors also presented wavelength-dependent circular polarization measurements ($\lambda\lambda 4000\text{--}9000$ Å) and discussed a simplified model based on a constant B (Planck function) gradient atmosphere. They found a discrepancy of a factor of 4 between the mean longitudinal field deduced from the spectrum (based on a centred dipole model) and the continuum polarization data, the latter being found smaller.

The multichannel spectrophotometry of G 99-47 yields an effective blackbody temperature of 5700 K (Greenstein 1974). We proceed on the assumption that G 99-47 has a nearly pure hydrogen atmosphere ($\text{He}/\text{H} = 0.1$) and use as our basic model a $T_e = 6000$ K, $\log g = 8.0$ DA model atmosphere obtained from Wickramasinghe *et al.* (1977). We expect our conclusions to be fairly insensitive to the helium abundance provided $\text{He}/\text{H} \lesssim 10$. The model has a metal abundance of 10^{-3} times the solar value, consistent with the non-detectability of metal lines for a nonmagnetic DA white dwarf at $T_e = 6000$ K.

Sequences of centred dipole models were constructed for polar field strengths $B_d = 2 \times 10^7$ G and 2.5×10^7 G, the possible values suggested by Liebert *et al.* (1975). The computed

Table 3. Model predictions for G 99-47.

B_d (gauss)	d/R	i ($^\circ$)	V_1 ($\lambda\lambda$ 3500– 5500 Å) (per cent)	V_2 ($\lambda\lambda$ 4800– 5500 Å) (per cent)	V_3 ($\lambda\lambda$ 6020– 6380 Å) (per cent)	V_4 ($\lambda\lambda$ 6740– 7000 Å) (per cent)
2×10^7	0	180	0.80	0.74	1.59	-0.67
		150	0.69	0.64	1.45	-0.58
		135	0.56	0.52	1.22	-0.56
		120	0.39	0.36	0.86	-0.46
		90	0	0	0	0
2.5×10^7	0	180	0.99	0.92	1.69	-0.25
		150	0.85	0.80	1.55	-0.25
		135	0.69	0.65	1.32	-0.42
		120	0.49	0.46	0.96	-0.42
		90	0	0	0	0

mean values of V over several wavelength bands are given in Table 3. The values V_3 and V_4 should correspond closely to the observed 360 Å wide bands of high (0.95 ± 0.15 per cent) and low (-0.28 ± 0.15 per cent) circular polarization approximately coincident with the σ^- and σ^+ absorption bands of $H\alpha$, discussed by Liebert *et al.* (1975). It is interesting to compare our more accurate results with those of Liebert *et al.* for corresponding models. We compute a mean continuum polarization of 0.59 per cent for the V_3 (6020–6380 Å) band for $B_d = 2 \times 10^7$ G and $i = 150^\circ$, which implies a line contribution of 0.86 per cent (from Table 3). This should be compared with the value of 0.50 per cent quoted by Liebert *et al.* (1975) for the same model parameters.

The best-fitting centred dipole model based on wavelength agreement with the $H\alpha$ feature, continuum polarization and line polarization has parameters $B_d = 2.5 \times 10^7$ G, $i = 120^\circ$. The sign of polarization requires the negative pole to be pointing towards the observer. The observed values of polarization, namely V_1^{obs} (3500–5500 Å) = 0.45 per cent (Angel & Landstreet 1972), V_3^{obs} (6020–6380 Å) = 0.95 ± 0.15 per cent and V_4^{obs} (6740–7120 Å) = -0.28 ± 0.15 per cent (Liebert *et al.* 1975) are in remarkably close agreement with the computed values for this model (Table 3), contrary to the conclusions of Liebert *et al.* (1975). We find no significant discrepancy between observed and theoretical values of continuum polarization computed on the assumption that H^- is the main source of dichroism.

A comparison of the theoretical and observed spectrum over the wavelength region $\lambda\lambda$ 4000–7000 Å is given in Fig. 9. We note that our results indicate that $H\beta$ will not be detectable spectroscopically due to magnetic broadening, consistent with observations (Greenstein *et al.* 1971). The computed $H\alpha$ profile appears to be somewhat weaker than observed, but the overall agreement is satisfactory. Better agreement may be achieved by the inclusion of self-broadening which was recently shown to be an important source of line broadening in cool DA white dwarfs (Wickramasinghe & Bessell 1979). As in GD 90, the possibility that the magnetic field influences the structure of the atmosphere cannot be ruled out, although clearly increased blanketing will not be an important effect. Stronger lines will also result from the use of a higher effective temperature, but this appears unlikely in view of Greenstein's (1974) data.

3.3 BPM 25114

In a previous paper (Martin & Wickramasinghe 1978) we showed that theoretical spectra computed for a centred dipole model with $B_d = 3.6 \times 10^7$ G yielded results which were in

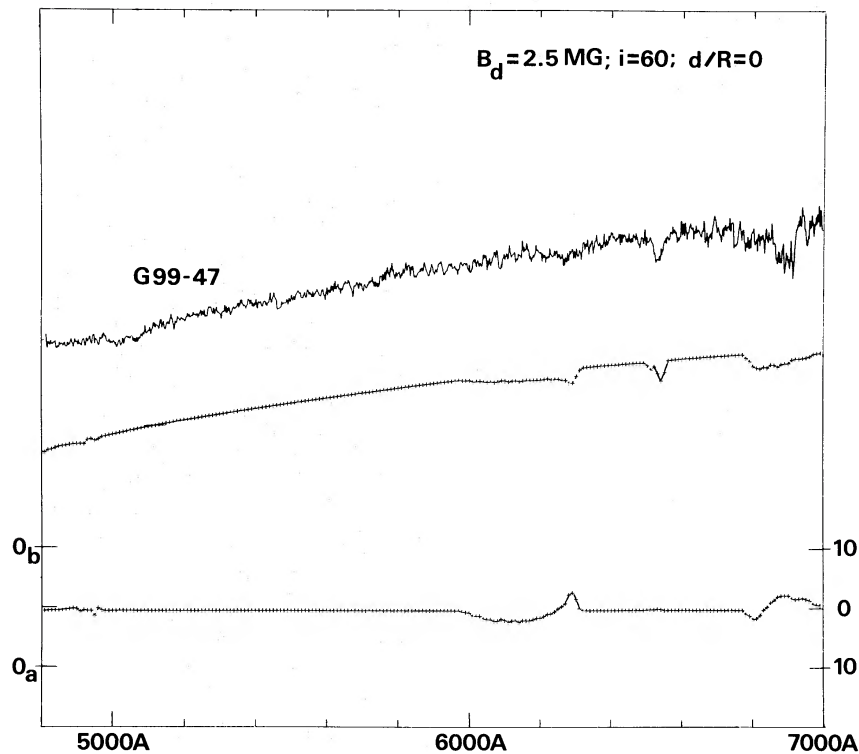


Figure 9. Observed and theoretical fluxes f_{ν} for G 99-47. There are two sets of values presented: (a) a model 6000 K magnetic white dwarf, dipole strength $B_d = 2.5$ MG, viewing angle $i = 60^\circ$, centred dipole ($d/R = 0$); (b) observations of magnetic DA white dwarf G 99-47 from Liebert *et al.* (1975). The top two curves represent flux for (a) and (b), from the bottom up respectively; the zeros of these are indicated on the left (0_a , 0_b). The flux of (a) is normalized in the continuum to that of (b). Circular polarization for (a) is represented by the bottom curve; the scale on the right has units of per cent, with positive polarization upwards. If the viewing angle is $i = 120^\circ$ (as indicated by observations of circular polarization and discussed in the text) instead of $i = 60^\circ$, the flux is unchanged and the sign of the circular polarization is reversed.

reasonable agreement with the spectrophotometric observations of BPM 25114. These results were based on a numerical technique which was tested on a grey temperature distribution, but was found later to give inaccurate results in the cores of strong lines in non-grey atmospheres. We have recomputed these models using the new numerical technique (Martin & Wickramasinghe 1979b) adopted in this paper, and find that our results at $H\alpha$ need to be modified somewhat. The new results are compared with observations in Fig. 10, and predicted mean values of V are given in Table 4. These results appear to be in better agreement with observations at $H\alpha$. Possible explanations for the differences which exist

Table 4. Model predictions for BPM 25114.

B_d (gauss)	d/R	i ($^\circ$)	$\bar{V}(\lambda\lambda 3500-5500 \text{ \AA})$ (per cent)
3.6×10^7	0	0	-0.55
		22.5	-0.51
		45.5	-0.40
		67.5	-0.22
		90.0	0

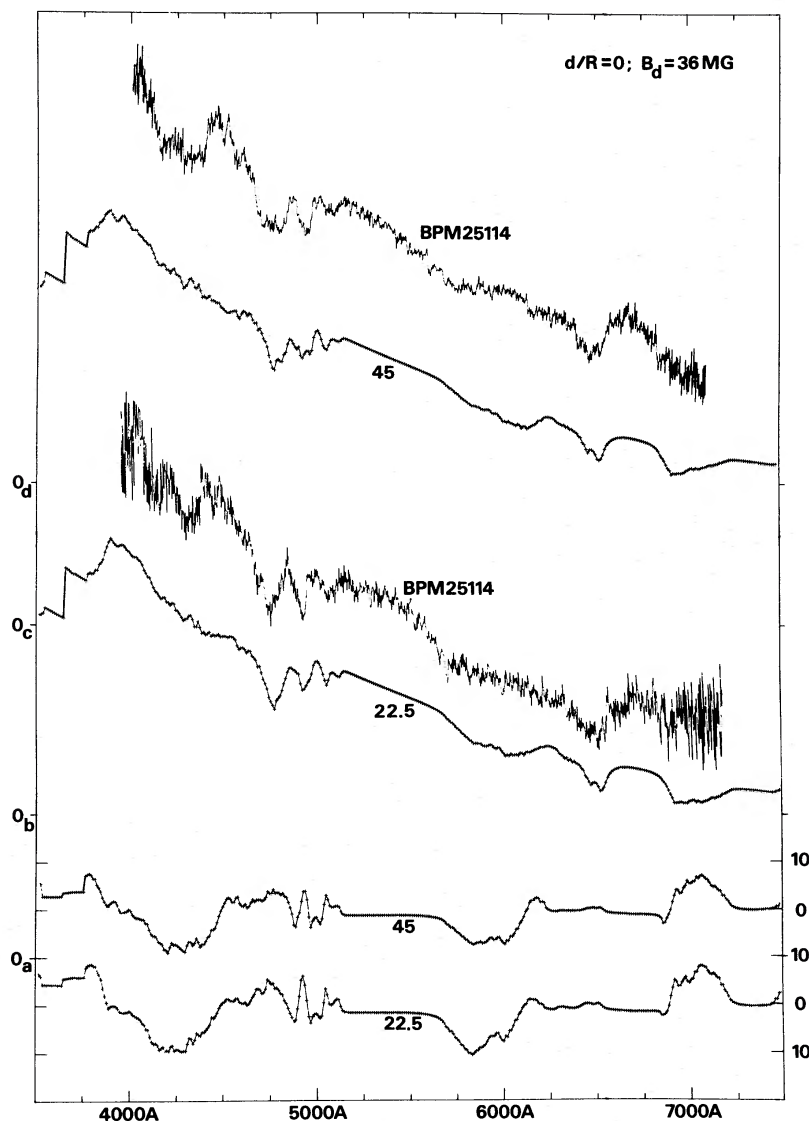


Figure 10. Observed and theoretical fluxes for BPM 25114. There are four sets of values presented: (a) a model 20 000 K magnetic white dwarf, dipole strength $B_d = 36$ MG, viewing angle $i = 22.5^\circ$, centred dipole ($d/R = 0$); (b) observations of magnetic DA white dwarf BPM 25114 from Wickramasinghe *et al.* (1977); (c) a model identical to (a) except $i = 45^\circ$; (d) observations of BPM 25114 made at a different time. The top four curves represent (a) to (d), from the bottom up respectively; the zeros of these curves are indicated on the left (0_a to 0_d). The fluxes of (a) and (c) are normalized to those of the observations in the continuum. Circular polarization for (a) and (c) are represented by the bottom two curves; the scale on the right has units of per cent, with positive polarization upwards.

between theory and observations of BPM 25114 have been discussed in Martin & Wickramasinghe (1978). As a result of our experience with GD 90, we consider the following additional factors as also being possibly important.

First, it may be unreasonable to expect better wavelength agreement than has already been achieved for $H\alpha$ and $H\beta$, since the interpolation procedure in Kemic's (1974a) tables will clearly introduce errors. This would apply particularly to rapidly moving components such as those which constitute the σ^- absorption band of $H\alpha$. The lack of detailed agreement in this wavelength region need not necessarily imply a radical departure from a dipole field geometry. Secondly, as in GD 90, increased blanketing could result in deeper lines as appears

to be required by observations. Until polarization data become available, a more detailed analysis of this star does not appear to be warranted.

4 Conclusions

We have analysed the spectrophotometric data and the available circular polarization data on the three known magnetic DA white dwarfs GD 90, G 99-47 and BPM 25114 using models which incorporate non-grey atmospheres and a full solution to the radiative transfer equations. Several important results have emerged from this investigation.

(1) We find that centred or off-centred dipole field geometries are in general adequate to interpret the observed spectra of magnetic DA white dwarfs. The lack of detailed agreement with the observed wavelengths of some of the features is likely to be caused by errors introduced by interpolation in the existing, rather coarsely spaced, tables for computing the Zeeman effect for hydrogen.

(2) Contrary to the conclusions of some previous investigators (Liebert *et al.* 1975; Angel 1978), we find good agreement between the theoretical values of continuum polarization and observations of GD 90 and G 99-47. These results suggest that it is adequate to use zero-field model atmospheres together with the existing theory for magnetoabsorption by H, He (Lamb & Sutherland 1974; Kemp 1977) and H^- (Angel 1977) for the analysis of continuum polarization data, at least for field strengths $B_d \lesssim 2.5 \times 10^7$ G. We note in particular that the present results indicate that we have no reason to doubt the validity of the rigid wave function assumption which is used in determining the magnetic circular dichroism of H^- .

(3) There is some evidence from the cores of absorption features, particularly in GD 90, to suggest that the magnetic field has an influence on the structure of the atmosphere. This may result directly from magnetic pressure or indirectly through line blanketing caused by absorption in the Zeeman components. Thus, the use of zero-field model atmospheres must be looked upon as a first approximation.

The success we have had in modelling the spectra of magnetic DA white dwarfs must be considered as strong astrophysical evidence in support of the Zeeman theory of hydrogen (Kemic 1974b; Garstang 1977) up to field strengths of $\approx 4 \times 10^7$ G. This is particularly important since at the present time such high fields cannot be easily realised under laboratory conditions. The self-consistent method of analysis presented in this paper appears adequate for a coarse analysis of magnetic white dwarfs, but refinements will have to be introduced when more detailed observations become available, particularly in the lines.

Acknowledgments

One of us (DTW) acknowledges support from the Australian Research Grants Committee.

References

- Angel, J. R. P., 1977. *Astrophys. J.*, **216**, 1.
 Angel, J. R. P., 1978. *A. Rev. Astr. Astrophys.*, **16**, 487.
 Angel, J. R. P., Carswell, R. F., Strittmatter, P. A., Beaver, E. A. & Harms, R., 1974. *Astrophys. J.*, **194**, L49.
 Angel, J. R. P. & Landstreet, J. D., 1972. *Astrophys. J.*, **178**, L21.
 Borra, E. F., 1976. *Astrophys. J.*, **209**, 858.
 Brown, D. N., Rich, A., Williams, W. L. & Vauclair, G., 1977. *Astrophys. J.*, **218**, 227.
 Eggen, O. J., 1968. *Astrophys. J. Suppl.*, **16**, 97.

- Garstang, R. H., 1977. *Rep. Prog. Phys.*, **40**, 105.
- Greenstein, J. L., 1974. *Astrophys. J.*, **194**, L51.
- Greenstein, J. L., Gunn, J. & Kristian, J., 1971. *Astrophys. J.*, **169**, L63.
- Griem, H., 1964. *Plasma Spectroscopy*, McGraw-Hill, New York.
- Kemic, S. B., 1974a. *Joint Institute Laboratory Astrophysics Report 113*.
- Kemic, S. B., 1974b. *Astrophys. J.*, **193**, 213.
- Kemp, J. C., 1977. *Astrophys. J.*, **213**, 794.
- Lamb, F. K. & Sutherland, P. G., 1974. *Physics of Dense Matter*, p. 265, ed. Hansen, C. J., D. Reidel, Dordrecht, Holland.
- Liebert, J., Angel, J. R. P. & Landstreet, J. D., 1975. *Astrophys. J.*, **202**, L139.
- Liebert, J., Angel, J. R. P., Stockman, H. S., Spinrad, H. & Beaver, E. A., 1977. *Astrophys. J.*, **214**, 457.
- Martin, B. & Wickramasinghe, D. T., 1978. *Mon. Not. R. astr. Soc.*, **183**, 533.
- Martin, B. & Wickramasinghe, D. T., 1979a. *Mon. Not. R. astr. Soc.*, in press.
- Martin, B. & Wickramasinghe, D. T., 1979b. *Mon. Not. R. astr. Soc.*, submitted.
- Shipman, H., 1971. *Astrophys. J.*, **167**, 165.
- Wegner, G., 1977. *Mem. Soc. astr. Ital.*, **48**, 27.
- Wickramasinghe, D. T., 1972. *Mem. R. astr. Soc.*, **76**, 129.
- Wickramasinghe, D. T. & Bessell, M. S., 1976. *Astrophys. J.*, **203**, L39.
- Wickramasinghe, D. T. & Bessell, M. S., 1979. *Mon. Not. R. astr. Soc.*, **186**, 399.
- Wickramasinghe, D. T., Cottrell, P. L. C. & Bessell, M. S., 1977. *Astrophys. J.*, **217**, L65.
- Wickramasinghe, D. T. & Martin, B., 1978. *Proc. astr. Soc. Aust.*, **3**, 269.
- Wickramasinghe, D. T., Whelan, J. & Bessell, M. S., 1977. *Mon. Not. R. astr. Soc.*, **180**, 373.